A Monte Carlo approach for the fully probabilistic evaluation of operability in ship dynamic positioning scenarios

Nabergoj, Radoslav; Mauro, Francesco

DOI
10.1063/5.0163317

Publication date
2023

Document Version
Final published version

Published in
AIP Conference Proceedings

RESEARCH ARTICLE | SEPTEMBER 28 2023

A Monte Carlo approach for the fully probabilistic evaluation of operability in ship dynamic positioning scenarios

Radoslav Nabergoj; Francesco Mauro

AIP Conf. Proc. 2872, 120090 (2023)
https://doi.org/10.1063/5.0163317

A Monte Carlo Approach for the Fully Probabilistic Evaluation of Operability in Ship Dynamic Positioning Scenarios

Radoslav Nabergoj[1, a)] and Francesco Mauro[2, 3, b)]

[1)]NASDIS PDS d.o.o., Industrijska Cesta 2e, Izola, 6310, Slovenija.
[2)]The Maritime Safety Research Centre, Department of Naval Architecture, Ocean and Marine Engineering (NAOME), University of Strathclyde, 100 Montrose St., Glasgow, G4 0LZ, Scotland, UK.
[3)]Department of Maritime and Transport Technology, Faculty of Mechanical, Maritime and Materials Engineering, Delft University of Technology, Leeghwaterstraat 17, 2628 CA Delft, the Netherlands

[a)]Corresponding author: radoslav.nabergoj@nasdispds.com
[b)]F.Mauro@tudelft.nl

Abstract. The Dynamic Positioning system allows a vessel to keep a precise position and heading during stationing operations in a rough sea by using onboard actuators only. During the design phase, it is mandatory to identify the capability of the system actuators to counteract the environmental forces. Conventional predictions are limited to the estimation of a maximum sustainable wind speed on predefined encounter angles by estimating the corresponding wave parameters with questionable standard deterministic correlations. The proposed approach aims at determining the dynamic positioning performances by using site-specific long-term environmental conditions which are modelled with joint distributions of wind and wave parameters. To this end, the operability of the dynamic positioning system is evaluated as a non-deterministic multidimensional Monte Carlo integration process, based on the sampling of environmental joint distributions. For each environmental condition, a quasi-static dynamic positioning analysis is performed solving the equilibrium between external forces and the vessel's actuators through a non-linear thrust allocation algorithm. The proposed methodology is applied to a reference offshore ship in five different operative geographic areas, highlighting the suitability of the calculation methodology for site-specific operability predictions.

INTRODUCTION

The Dynamic Positioning (DP) characteristics determination for a ship requires the knowledge of reference or site-specific environmental conditions. During the preliminary design phase, the description of the DP working environment of the vessel is not always correctly considered, as the methods usually employed to perform DP calculations only allow for the usage of fixed prescribed environmental conditions [1, 2, 3]. Such conditions are just deterministic wind-wave correlations, providing wave parameters (significant wave height H_s and peak period T_p) and wind speed V_w specific for reference DP predictions. These correlations allow for determining of a maximum wind speed envelope bounding the wind speed domain at each heading angle χ where the DP system holds the position [4]. However, there are different environmental characteristics descriptions for specific sea areas, giving a more detailed characterisation between the occurrence and correlations of wind and wave parameters [5]. Such models are potentially available since the preliminary phases of design but require the adoption of alternative calculation processes to assess DP system performances.

An alternative to conventional DP predictions is a quasi-probabilistic method developed to handle the joint occurrence of wave parameters H_s and T_p. This methodology, called the *scatter diagram approach* [6], considers the couples (H_s, T_p) present in the long-term statistic of a sea area (the scatter diagram) and uses a deterministic procedure to evaluate the wind speed V_w from H_s and T_p occurrence. Therefore, the DP calculations refer to the cells of a scatter diagram. As the main relevant output, the *scatter diagram approach* does not produce a limiting wind speed envelope but calculates the DP system operability in a given sea area. This is a shortcut for the designers.

Nonetheless, it is possible to reproduce the long-term environmental conditions of a given sea area also considering the joint occurrence of wind and waves [7], thus employing a trivariate joint distribution of V_w, H_s and T_p. A specific and fully probabilistic description of the environmental parameters does not allow evaluating DP system operability through calculations on specific predetermined conditions. Here, a novel approach calculates the operability as numerical integration, implementing a Monte Carlo (MC) process for DP performance estimation. The implemented procedure samples the environmental conditions from the joint distribution, which are the inputs for DP calculations. In this study, the DP analysis follows a quasi-static approach. That means solving the equilibrium between external forces and vessel actuators through a thrust allocation algorithm. The proposed MC procedure uses a non-linear thrust allocation algorithm [8] to solve the quasi-static problem. The paper reports the application of the MC process to a reference vessel for different operative sea areas of interest. The study analyses the integration convergence and the

11th International Conference on Mathematical Modeling in Physical Sciences
AIP Conf. Proc. 2872, 120090-1–120090-12; https://doi.org/10.1063/5.0163317
Published by AIP Publishing. 978-0-7354-4657-1/$30.00

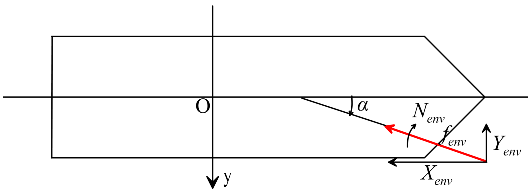

FIGURE 1. Reference system for quasi-static DP analysis.

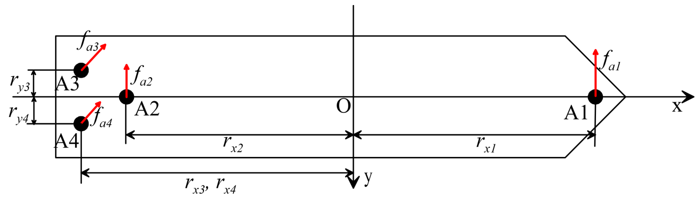

FIGURE 2. Actuators layout for the reference OSV.

TABLE I. Reference OSV main characteristics.

Name	Symbol		Unit
Length between perpendiculars	L_{PP}	72.00	m
Length overall	L_{OA}	78.35	m
Maximum breadth	B	16.00	m
Operative draught	T	4.05	m
Volume	∇	3245.21	m^3
Lateral exposed wind area	A_L	854.10	m^2
Transversal exposed wind area	A_T	187.40	m^2

TABLE II. Reference OSV actuators configuration.

Actuator ID and type	r_x (m)	r_y (m)	$f_{a_{max}}$ (kN)
A1 (*tunnel thruster*)	32.00	0.00	73.50
A2 (*tunnel thruster*)	−30.00	0.00	62.50
A3 (*azimuth thruster*)	−36.00	−3.00	240.00
A4 (*azimuth thruster*)	−36.00	3.00	240.00

variance of the results introduced by the MC process on the DP operability. The results allow identifying a suitable confidence interval for the operability determination, including the heading angle χ in the sampling process.

QUASI-STATIC DP ANALYSIS

Two different methods allow for evaluating the stationing capability of offshore ships: quasi-static analysis [9, 10] and time-domain simulations [11, 12]. The latter method is more time-consuming and requires knowledge of the control parameters of the effective DP system installed onboard the analysed ship [13]. Therefore, time-domain simulations are particularly suitable for the final assessment of DP performances for the definitive system mounted onboard. On the other hand, quasi-static calculations are the preferred option when all the ship and DP system parameters are not fixed or known, but an assessment of DP performances is needed. For such a reason, quasi-static DP analyses are a standard praxis in the design of offshore ships.

The so-called quasi-static analysis of the DP performances consists of the resolution of the static equilibrium of forces/moment acting on the ship's horizontal plane, which means primarily environmental and actuator loads taking into account dynamic effects with dynamic allowances on input loads. Considering, for instance, a body-fixed reference system centered at midship (see Figure 1), the static equilibrium in 3 degrees of freedom has the following form:

$$\boldsymbol{f}_{env} = \boldsymbol{A}(\boldsymbol{\alpha})\,\boldsymbol{f_a} \tag{1}$$

where $\boldsymbol{f}_{env} = [X_{env}, Y_{env}, N_{env}]^{\mathrm{T}}$ is the environmental loads vector, $\boldsymbol{f_a} = [f_{a_1}, \cdots, f_{a_{N_a}}]^{\mathrm{T}}$ is the vector of the thrust delivered by the N_a actuators and $\boldsymbol{A}(\boldsymbol{\alpha}) \in \mathbb{R}^{3\times N_a}$ is a matrix containing the actuator positions and the thrust orientations vector $\boldsymbol{\alpha} = [\alpha_1, \cdots, \alpha_{N_a}]^{\mathrm{T}}$. The definition of $\boldsymbol{A}(\boldsymbol{\alpha})$ is vessel-specific and depends on the type of actuators installed onboard. Considering $\boldsymbol{A}(\boldsymbol{\alpha})$ as a set of N_a column vectors $\boldsymbol{a_i} \in \mathbb{R}^3$, the following forms apply to the actuators commonly used for DP purposes:

$$\boldsymbol{a}_i = \begin{cases} [1, 0, -r_{y_i}]^{\mathrm{T}} & \text{for main propellers} \\ [0, 1, r_{x_i}]^{\mathrm{T}} & \text{for fixed tunnel thusters or rudders} \\ [\cos\alpha_i, \sin\alpha_i, r_{x_i}\sin\alpha_i - r_{y_i}\cos\alpha_i]^{\mathrm{T}} & \text{for azimuth thusters} \end{cases} \tag{2}$$

where r_{x_i} and r_{y_i} are the transversal and longitudinal positions of the onboard actuators.

The present study uses as a reference an offshore supply vessel (OSV) having the main dimensions and actuators configuration reported in Table I and Table II, respectively. The actuator layout is also shown in Figure 2. The reference OSV has two steerable and two fixed tunnel thrusters as actuators. Therefore, remembering actuators definition given in Eq. (2), matrix $\boldsymbol{A}(\boldsymbol{\alpha}) \in \mathbb{R}^{3\times 4}$ assumes the following form:

$$\boldsymbol{A}(\boldsymbol{\alpha}) = \begin{bmatrix} 0 & 0 & \cos\alpha_3 & \cos\alpha_4 \\ 1 & 1 & \sin\alpha_3 & \sin\alpha_4 \\ r_{x_1} & r_{x_2} & r_{x_3}\sin\alpha_3 - r_{y_3}\cos\alpha_3 & r_{x_4}\sin\alpha_4 - r_{y_4}\cos\alpha_4 \end{bmatrix} \tag{3}$$

Then, the static equilibrium for the reference OSV results by substituting Eq. (3) in Eq. (1):

$$\begin{bmatrix} X_{env} \\ Y_{env} \\ N_{env} \end{bmatrix} = \begin{bmatrix} 0 & 0 & \cos\alpha_3 & \cos\alpha_4 \\ 1 & 1 & \sin\alpha_3 & \sin\alpha_4 \\ r_{x_1} & r_{x_2} & r_{x_3}\sin\alpha_3 - r_{y_3}\cos\alpha_3 & r_{x_4}\sin\alpha_4 - r_{y_4}\cos\alpha_4 \end{bmatrix} \begin{bmatrix} f_{a_1} \\ f_{a_2} \\ f_{a_3} \\ f_{a_4} \end{bmatrix} \tag{4}$$

The equilibrium system in Eq.4 has a number of unknowns N_u=6. The unknowns can be grouped in a reference vector $\boldsymbol{u} = [\boldsymbol{f_a}, \boldsymbol{\alpha}]^{\mathrm{T}} = [f_{a_1}, f_{a_2}, f_{a_3}, f_{a_4}, \alpha_3, \alpha_4]^{\mathrm{T}} \in \mathbb{R}^6$. As general rule, an azimuth thruster has 2 unknowns while tunnel thrusters, rudders and fixed propeller have one unknown each. Therefore, N_u can be determined for all vessel types and any actuators configuration as $N_u = N_a + N_{at}$, where N_{at} is the number of azimuth thrusters installed onboard. Hence, for quasi-static DP calculations, the resolution of Eq.(4) admits infinite solutions when $N_u > 3$. That means an unique solution of the equilibrium is admitted only in the case of unrealistic DP actuator layouts as a combination of 1 azimuth and 1 tunnel thrusters or the presence of 3 tunnel thrusters only. For such reasons, alternative solutions are needed to solve the equilibrium system.

Thrust allocation

The resolution of the static equilibrium system in Eq.(4) imply the implementation of a suitable algorithm to determine $\boldsymbol{u}$, means the proper distribution $\boldsymbol{f_a}$ and orientation $\boldsymbol{\alpha}$ of the thrust among the N_a actuators. The computation of $\boldsymbol{u}$ is adaptable to a constrained optimisation problem, minimising an approximated expression of the absorbed power as a function of $\boldsymbol{f_a}$:

$$\min(z) = \sum_{i=1}^{N_a} |f_{a_i}|^{3/2} \tag{5}$$

subject to the following constraints:

$$\boldsymbol{A}(\boldsymbol{\alpha})\,\boldsymbol{f_a} = \boldsymbol{f}_{env} \tag{6a}$$

$$\boldsymbol{f}_{a_{min}} \leq \boldsymbol{f_a} \leq \boldsymbol{f}_{a_{max}} \tag{6b}$$

$$\boldsymbol{\alpha}_{min} \leq \boldsymbol{\alpha} \leq \boldsymbol{\alpha}_{max} \tag{6c}$$

The constraints described by Eq.(6a) represents the static equilibrium system of Eq.(4), Eq.(6b) is used to allocate thrust between the actuator saturation limits, and Eq.(6c) sets the feasible sectors of azimuth angles α_i.

The optimisation problem provided by Eq.(5) and Eq.(6) is nonconvex and nonlinear and can be solved by using a nonlinear iterative optimisation algorithm [8]. Such a method, can handle the thrust allocation problem considering as unknowns $\boldsymbol{f_a}$ and $\boldsymbol{\alpha}$, or considering the thrust components $\boldsymbol{f}_{ax} = \boldsymbol{f_a}\cos\boldsymbol{\alpha}$ and $\boldsymbol{f}_{ay} = \boldsymbol{f_a}\sin\boldsymbol{\alpha}$, expressed in the body fixed reference system [14]. With this change of variables, the objective function remains nonlinear but Eq.(6a) becomes linear. The constraints of Eq.(6b) become nonlinear but can be easily linearised to reduce the resolution complexity without losing accuracy in the final result. The implementation of azimuth constraints in Eq.(6c) is substituted by automatically adding equality constraints when needed, forcing the actuator to stay in the feasible region.

As a results the thrust allocation algorithm determines, beside the specific thrust intensity and orientation of the actuators, whether the DP system is capable or not to keep the position, thus respecting the equilibrium of Eq.(1).

Environmental loads

The environmental loads $\boldsymbol{f}_{env}$ acting on the ship are the main external forces influencing the equilibrium needed to perform a quasi-static DP analysis. It is then necessary to analyse more in detail their evaluation. The conventional breakdown of the environmental forces is as follows:

$$\boldsymbol{f}_{env} = (\boldsymbol{f}_{wind} + \boldsymbol{f}_{wave} + \boldsymbol{f}_{curr})\, CA_{dyn} \tag{7}$$

where $\boldsymbol{f}_{wind} = [X_{wind}, Y_{wind}, N_{wind}]^{\mathrm{T}}$ are the wind loads, $\boldsymbol{f}_{wave} = [X_{wave}, Y_{wave}, N_{wave}]^{\mathrm{T}}$ are the wave loads and $\boldsymbol{f}_{curr} = [X_{curr}, Y_{curr}, N_{curr}]^{\mathrm{T}}$ are the current loads. CA_{dyn} is a dynamic allowance coefficient, which is an expedient to include dynamic effects in quasi-static DP predictions. Such coefficient can be derived from time-domain simulation on the same or similar ships or from guidelines provided by Classification Societies. Here, use has been made of a CA_{dyn}=1.25, as prescribed by DNV-GL [3].

The conventional formulations for environmental loads use non-dimensional coefficients as a function of the calculation heading angles vector χ. This approach allows for use the same coefficients on similar ships, without the need to assess with direct methods or model tests the loads. The application is straightforward for wind and current loads, leading to the following formulations:

$$\boldsymbol{f}_{wind} = \begin{bmatrix} X_{wind} \\ Y_{wind} \\ N_{wind} \end{bmatrix} = \frac{1}{2}\rho_{air} V_w^2 \begin{bmatrix} A_T \\ A_L \\ A_L L_{OA} \end{bmatrix} \boldsymbol{C}_{wind}(\chi) \tag{8}$$

$$\boldsymbol{f}_{curr} = \begin{bmatrix} X_{curr} \\ Y_{curr} \\ N_{curr} \end{bmatrix} = \frac{1}{2}\rho_{water} V_c^2 \begin{bmatrix} S \\ S \\ S L_{PP} \end{bmatrix} \boldsymbol{C}_{curr}(\chi) \tag{9}$$

where $\boldsymbol{C}_{wind} = [C_{X_w}, C_{Y_w}, C_{N_w}]^{\mathrm{T}}$ and $\boldsymbol{C}_{curr} = [C_{X_c}, C_{Y_c}, C_{N_c}]^{\mathrm{T}}$ are the wind and current non-dimensional coefficients, respectively. The other quantities in Eq.(8) and Eq.(9) are: ρ_{air} the air density, ρ_{water} the water density, V_w is the wind speed, V_c is the current speed, A_T is the transverse exposed area to wind, A_L is the lateral exposed area to wind, S is the hull wetted surface, L_{PP} is the length between perpendiculars and L_{OA} is the ship's overall length.

The wave forces require a different description of non-dimensional coefficients and calculation process compared to wind and current loads. For quasi-static DP calculations, the wave loads are described by means of mean drift forces, representative of an irregular and usually long-crested sea for specific couples of H_s and T_p. Mean drift forces can be measured through dedicated model scale experiments or derived from the quadratic transfer functions (QTF) calculated by diffraction theory. Then, modelling the irregular sea with a spectrum for a specific H_s and T_p values, the wave loads result in:

$$\boldsymbol{f}_{wave} = \begin{bmatrix} X_{wave} \\ Y_{wave} \\ N_{wave} \end{bmatrix} = \rho_{water} g \begin{bmatrix} \nabla^{\frac{1}{3}} \\ \nabla^{\frac{1}{3}} \\ \nabla^{\frac{2}{3}} \end{bmatrix} \int_0^{\infty} \boldsymbol{C}_{wave}(\chi, \boldsymbol{\omega})\, S_{\zeta}(\boldsymbol{\omega})\, \mathrm{d}\omega \tag{10}$$

where $\boldsymbol{C}_{wave} = [C_{X_{wav}}, C_{Y_{wav}}, C_{N_{wav}}]^{\mathrm{T}}$ represent the QTF as a function of the heading angle vector χ and circular wave frequency vector $\boldsymbol{\omega}$. ∇ is the vessel volume of displacement, g the acceleration of gravity and S_{ζ} is the wave amplitude spectrum expressed as a function of circular wave frequency vector $\boldsymbol{\omega}$.

From the given description of environmental loads it results that a single resolution of Eq.(5) optimisation problem requires the definition of a tuple of environmental parameters $\boldsymbol{e} = [V_w, V_c, H_s, T_p, \chi]^{\mathrm{T}}$ to describe the external loads. This is valid assuming that the environmental loads are concurrent within each other, as common practice for quasi-static calculations. Another simplification for quasi-static analysis concerns the current speed V_c, which is supposed to be constant through all the combination of other environmental parameters. In this study, V_c=0.75 m/s is used as reference value for current loads.

DP operability

The conventional quasi-static analysis considers fixed combinations of wind speed and wave parameters through a deterministic relationship. The adoption of such kind of environment definition leads to the determination of the so-called DP system capability through consecutive quasi-static calculations monotonically increasing V_w. The capability

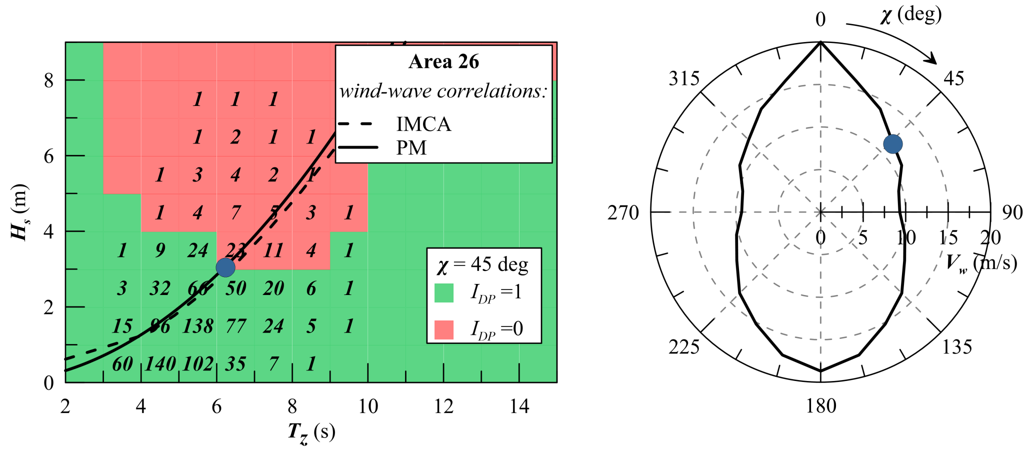

FIGURE 3. Scatter diagram approach representation for one heading χ and correlation with a DP capability plot.

represents the maximum sustainable wind speed $V_{w_{max}}$ the DP system can face, using the on-board actuators, at each heading angle χ. The obtained $V_{w_{max}}$ as a function of χ is then reported in a conventional polar plot called Capability Plot. To capture all the possible combinations of wave parameters occurring in sea area, an alternative method is necessary.

A valid methodology is provided by the scatter diagram approach [6]. Instead of performing basic DP capability plot predictions, the scatter diagram approach allows the execution of DP calculations for each combination of H_s and T_p of the operational area. Calculations can be carried out for the heading vector χ, evaluating whether the DP system is able or not to keep the vessel in position with the resulting sea environment. This strategy allows for a novel evaluation of the DP system performances on a specific sea environment, enhancing the concept of DP capability in favor of the direct quantitative evaluation of the operability of the system. The operability results from the following formulation:

$$OP_{DP} = \sum_{i=1}^{N_\chi} f_{\chi_i} \sum_{j=1}^{N_{H_s}} \sum_{k=1}^{N_{T_p}} f_{w_{jk}} I_{DP_{ijk}} \tag{11}$$

where $\boldsymbol{f}_\chi = [f_{\chi_1}, \cdots, f_{\chi_{N_\chi}}]^\mathrm{T} \in \mathbb{R}^{N_\chi}$ is the occurrence of the N_χ headings considered in the calculation, $\boldsymbol{f}_w = [f_{w_{11}}, \cdots, f_{w_{1N_{T_p}}}; \cdots; f_{w_{N_{H_s}1}}, \cdots, f_{w_{N_{H_s}N_{T_p}}}]^\mathrm{T} \in \mathbb{R}^{N_{H_s} \times N_{T_p}}$ is the joint occurrence of H_s and T_p, provided by a scatter diagram having a granularity of N_{H_s} wave heights and N_{T_p} wave periods. The last element to define in Eq.(11) is the matrix $\boldsymbol{I}_{DP} \in \mathbb{R}^{N_{H_s} \times N_{T_p}}$, which is containing the results of the single quasi-static analysis on the scatter diagram cells in the following form:

$$I_{DP_{ijk}} = \begin{cases} 1 & \text{if a feasible solution to optimisation problem in Eq.(5) exsist (the DP system holds position)} \\ 0 & \text{otherwise} \end{cases} \tag{12}$$

However, a scatter diagram covers only combinations of wave parameters (H_s and T_p), without giving information concerning wind speed V_w. The discrete nature of Eq.(11) favors the evaluation of a single V_w for each cell of the scatter diagram, adopting a deterministic and simplified procedure derived from the Pierson-Moskowitz wave spectrum [15]. Such simplification allows for fast evaluation of OP_{DP}, however does not properly take into account the statistic of V_w in the geographic sea area. Figure 3 shows an example of results provided with a scatter diagram approach and its correlation with the DP capability plots obtained with Pierson-Moskowitz wind-wave correlation.

ENVIRONMENTAL MODELING WITH TRIVARIATE JOINT DISTRIBUTIONS

The process described by the scatter diagram approach can be enhanced by changing the description of the area-specific long-term environmental conditions. The availability of environmental data derived from local measurements or forecast models allows the definition of joint probability distributions for wind and waves. In the specific, dealing with the necessity to define V_w, H_s and T_p a trivariate joint distribution should be defined.

A possible formulation for the probability density function of a trivariate joint V_w-H_s-T_p distribution is as follows:

$$f_{V_w,H_s,T_p}\left(v_w,h_s,t_p\right) = f_{V_w}\left(v_w\right) f_{H_s|V_w}\left(h_s,v_w\right) f_{T_p|V_w,H_s}\left(t_p,h_s,v_w\right) \tag{13}$$

where v_w, h_s and t_p are three random variables in $(0,+\infty)$ needed to define the joint distribution. Eq.(13) is composed by a marginal distribution f_{V_w} for the wind speed, a conditional distribution $f_{H_s|V_w}$ for the wave height and another conditional distribution $f_{T_p|V_w,H_s}$ for the wave period. The marginal distribution for V_w can be modelled with a two parameters Weibull distribution [5]:

$$f_{V_w}\left(v_w\right) = \frac{\beta_v}{\eta_v}\left(\frac{v_w}{\eta_v}\right)^{\beta_v-1} \mathrm{e}^{-\left(\frac{v_w}{\eta_v}\right)^{\beta_v}} \tag{14}$$

where β_v and η_v are the shape and scale parameter of the distribution, which are varying depending on the geographic site environmental statistics. A two parameters Weibull model can be employed also for the conditional f_{H_s,V_w} distribution:

$$f_{H_s|V_w}\left(h_s,v_w\right) = \frac{\beta_h}{\eta_h}\left(\frac{h_s}{\eta_h}\right)^{\beta_h-1} \mathrm{e}^{-\left(\frac{h_s}{\eta_h}\right)^{\beta_h}} \tag{15}$$

This formulation is analogue to Eq.(14), but shape and scale parameters are modelled as power functions of v_w as follows:

$$\beta_h = a_1 + a_2 {v_w}^{a_3} \tag{16a}$$

$$\eta_h = b_1 + b_2 {v_w}^{b_3} \tag{16b}$$

such modelling grants the dependence of Eq.(15) from both v_w and h_s.

The conditional distribution $f_{T_p|H_s,V_w}$ is usually modelled with a log-normal distribution:

$$f_{T_p|H_s,V_w}\left(t_p,h_s,v_w\right) = \frac{1}{\sqrt{2\pi}\sigma_{T_p} t_p} \mathrm{e}^{-\frac{1}{2}\left(\frac{\ln t_p - \mu_{T_p}}{\sigma_{T_p}}\right)^2} \tag{17}$$

where the standard deviation σ_{T_p} and the mean value μ_{T_P} of $\ln t_p$ are expressed with the following functions of v_w and h_s:

$$\mu_{T_p} = \ln \frac{\mu^*_{T_p}}{\sqrt{\nu^2_{T_p}+1}} \tag{18a}$$

$$\sigma_{T_p} = \sqrt{\ln\left(\nu^2_{T_p}+1\right)} \tag{18b}$$

$$\nu_{T_p} = c_1 + c_2 \mathrm{e}^{c_3 h_s} \tag{18c}$$

$$\mu^*_{T_p} = \overline{T_p}\left[1+\theta\left(\frac{v_w-\overline{v_w}}{\overline{v_w}}\right)^{\gamma}\right] \tag{18d}$$

$$\overline{T_p} = d_1 + d_2 h_s^{d_3} \tag{18e}$$

$$\overline{v_w} = e_1 + e_2 h_s^{e_3} \tag{18f}$$

Such modelling of the trivariate joint distribution with Eq.(14), Eq.(15) and Eq.(17) requires the definition of a set of parameters $\boldsymbol{q} = [\eta_v, \beta_v, a_1, a_2, a_3, b_1, b_2, b_3, c_1, c_2, c_3, d_1, d_2, d_3, e_1, e_2, e_3, \theta, \gamma]^{\mathrm{T}}$ which are site-specific and determined by fitting procedures on environmental data.

Employing and environmental modelling with Eq.(13) does not allow anymore to have unique combinations of V_w, H_s and T_p, necessary to apply the scatter diagram approach and evaluate OP_{DP} according to Eq.(11). It is then necessary to develop a different method for the DP operability evaluation with joint distributions of environmental parameters.

DP OPERABILITY AS A MONTE CARLO PROCESS

The adoption of the previously described enhanced environmental modelling with trivariate joint distributions requires a different approach to DP operability calculation. A possible solution is evaluate DP operability as a non-deterministic multidimensional Monte Carlo (MC) integration. An approximated MC integral has the following formulation:

$$\int_{\Omega} f(\boldsymbol{x})\,\mathrm{d}\boldsymbol{x} \approx \frac{1}{N_s}\int_{\Omega}\mathrm{d}\boldsymbol{x}\sum_{i=1}^{N_s} f(\boldsymbol{x}_i) \tag{19}$$

where $\Omega \in \mathbb{R}^m$ is an m-dimensional probability space, $\boldsymbol{x} \in \Omega$ is a matrix of m independent random variables having N_s elements each. In case Ω is an unit hypercube $(0,1)^m$, then the term $\int_{\Omega}\mathrm{d}\boldsymbol{x}$ in Eq.(19) is equal to 1. Then, considering uniform random variables $\boldsymbol{U} \sim \mathbb{U}(0,1)$, Eq.(19) can be rewritten as:

$$\int_{\Omega} f(\boldsymbol{x})\,\mathrm{d}\boldsymbol{x} \approx \frac{1}{N_s}\sum_{i=1}^{N_s} f(\boldsymbol{U}_i) \tag{20}$$

Using the trivariate joint distribution in Eq.(13) and modelling v_w, h_s and t_p as uniform random variables $\boldsymbol{U}$, Eq.(11) can be adapted to an MC integral formulation:

$$OP_{DP} = \sum_{i=1}^{N_\chi} f_{\chi_i}\frac{1}{N_s}\sum_{j=1}^{N_s} f_{V_w,H_s,T_p}\left(\boldsymbol{U}_{v_w},\boldsymbol{U}_{h_s},\boldsymbol{U}_{t_p}\right) I_{DP_j} \tag{21}$$

The OP_{DP} determination according to Eq.(21) maintains a discrete modelling of the heading angles, implying the resolution of a dedicated integration on each χ_i angle. Such procedure is useful if the OP_{DP} for specific headings is of interest. Otherwise, aiming at the determination of the global operability of the DP system, the modelling of the heeding can be also included in the integration process, considering an additional random variable. The MC integral can be than rewritten as:

$$OP_{DP} = \frac{1}{N_s}\sum_{i=1}^{N_s} f_{\chi}\left(\boldsymbol{U}_{\chi}\right) f_{V_w,H_s,T_p}\left(\boldsymbol{U}_{v_w},\boldsymbol{U}_{h_s},\boldsymbol{U}_{t_p}\right) I_{DP_i} \tag{22}$$

where f_χ is a probability density function of headings. The structure of Eq.(22) considers the heading distributions independent from the joint environmental parameters distribution. The evaluation of operability with Eq.(22) requires the evaluation of the tuple of environmental parameters previously introduced; however, being the current speed V_c fixed in the calculation assumption, the reduced tuple $\boldsymbol{e}^* = [V_w, H_s, T_p, \chi]^{\mathrm{T}}$ needs to be generated from the pertinent distributions. The procedure for MC integration uses a direct sampling from $\boldsymbol{U}$ with pseudo-random numbers [16], then, dealing with non-uniform distributions, the associated random variables are derived from the inversion of the reference cumulative density function. Considering a generic variable with cumulative F, being $\boldsymbol{U}$ uniform in $[0,1]$, the inverse $F^{-1}(\boldsymbol{U})$ is distributed according to F.

However, the adoption of pseudo-random numbers generates different combinations of parameters in $\boldsymbol{e}^*$ during each calculation, leading to different final integral values and convergence histories. As the approximated integral converges to an exact value as N_s increases without upper bounds, then the process is subject to uncertainties. It is then necessary to use a sufficiently large number of samples that ensures the matching of a required confidence level for the solution. This can be achieved by calculating a Confidence Interval (*CI*) across multiple repetitions N_r. In the next section the described process is applied to the reference OSV presented in next section for 5 different areas, introducing convergence criteria suitable for offshore operations.

MC PROCESS APPLICATION ON THE REFERENCE OSV

The above-described process is here applied on the reference OSV vessel. The first part of the process concerns the environmental modelling. In this example, 5 different geographic sea areas (*Area#1*, *Area#2*, *Area#3*, *Area#4* and *Area#5*) are considered, having the parameters $\boldsymbol{q}$ needed to define the trivariate distribution of Eq.(13) as listed in Table III. The areas are distributed across the European Atlantic coast and the North Sea and are relevant for the installation of offshore wind and waves energy devices [17].

TABLE III. Parameters $\boldsymbol{q}$ for the trivariate joint distribution on five reference geographic sea areas.

	f_{V_w} Eq.(14)		$f_{H_s\|V_w}$ Eq.(15)						$f_{T_p\|V_w,H_s}$ Eq.(17)										
Area	η_v	β_v	a_1	a_2	a_3	b_1	b_2	b_3	c_1	c_2	c_3	d_1	d_2	d_3	e_1	e_2	e_3	θ	γ
1	2.262	7.635	1.894	0.012	1.741	0.929	0.024	1.827	5.0	5.883	0.201	2.0	3.947	0.620	-0.002	0.341	-0.186	-0.268	1.0
2	2.002	7.866	1.643	0.093	1.000	1.963	0.031	1.644	5.0	5.970	0.223	1.0	4.055	0.466	0.030	0.234	-0.221	-0.143	1.0
3	2.050	7.859	2.044	0.034	1.375	1.323	0.032	1.757	8.0	2.600	0.409	1.8	3.478	0.667	0.002	0.298	-0.166	-0.233	1.0
4	2.029	9.409	2.136	0.013	1.709	1.816	0.024	1.787	8.0	1.938	0.486	2.5	3.001	0.745	-0.001	0.316	-0.145	-0.255	1.0
5	2.299	8.920	1.755	0.184	1.000	0.534	0.070	1.435	5.563	0.798	1.0	3.5	3.592	0.735	0.050	0.388	-0.321	-0.477	1.0

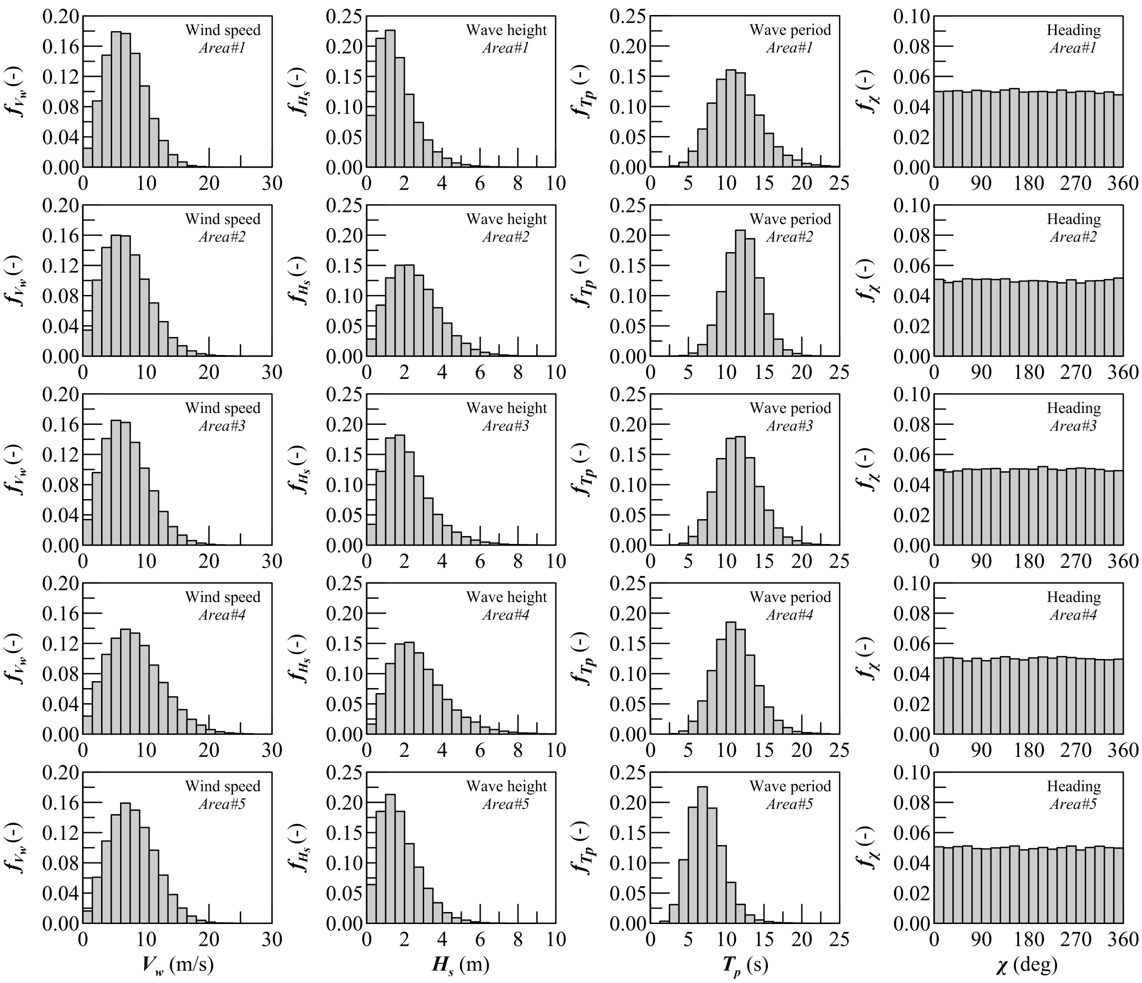

FIGURE 4. Marginal distributions of the environmental variables and heading angles generated for the 5 reference geographic sea areas.

However, the application of Eq.(22) to evaluate OP_{DP} for the reference OSV requires, besides the environmental conditions, to define the function f_χ describing the distribution of headings χ, and then determining $\boldsymbol{e}^*$ for the DP analyses. Here, the process is applied considering f_χ as a uniform random variable $\boldsymbol{U_\chi} \sim \mathbb{U}(0,1)$ independent from the three random variables v_w, h_s and t_p used for the trivariate joint distribution of environmental parameters. That means all the angles χ in [0,360] are considered equiprobable and independent from other simulation parameters.

Considering a sample size $N_s = 10^5$, the determination of $\boldsymbol{e}^*$ is performed according to the following steps:

1. Generation of $\boldsymbol{\Omega} = [\boldsymbol{U_\chi}, \boldsymbol{U}_{V_w}, \boldsymbol{U}_{H_s}, \boldsymbol{U}_{T_p}]^{\mathrm{T}}$ with pseudo-random number sequences with sample size N_s.

2. Direct determination of χ from $\boldsymbol{U_\chi}$.

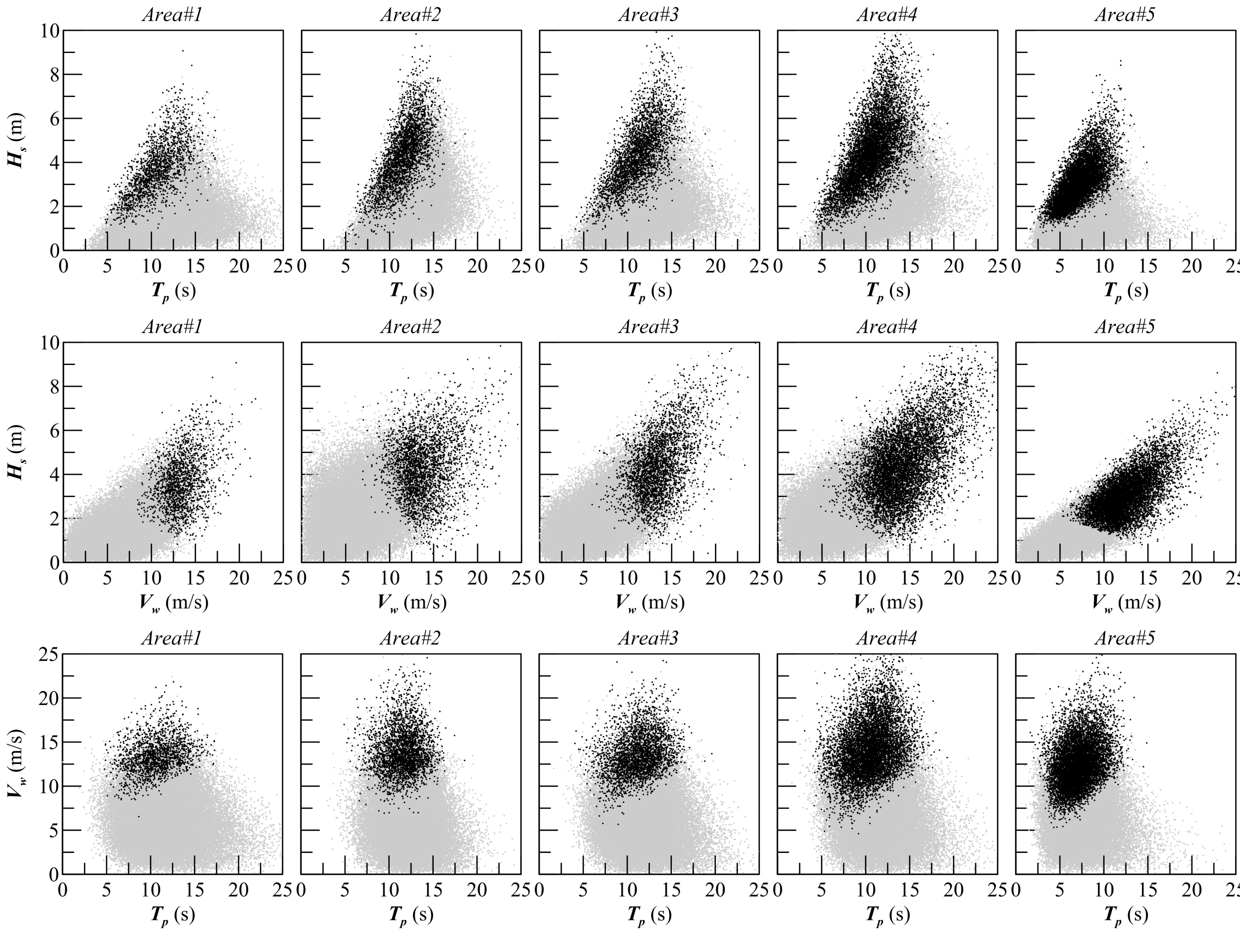

FIGURE 5. I_{DP} values as a function of $H_s - T_p$ (*top*), $H_s - V_w$ (*middle*) and $V_w - T_p$ (*bottom*) for the five reference areas.

3. Inversion of f_{V_w} (Eq.(14)) to obtain the wind speed random variable v_w.
4. Inversion of $f_{H_s|V_w}$ (Eq.(15)) using v_w to obtain the significant wave height random variable h_s.
5. Inversion of $f_{T_p|V_w,H_s}$ (Eq.(17)) using v_w and h_s to obtain the peak period random variable t_p.
6. Determination of $\boldsymbol{e}^*$ for all the N_s samples.

The results of the sampling process on the reference ship for the five geographic sea areas is presented in Figure 4. Here the marginal distributions of v_w, h_s, t_p and χ are reported in form of histograms. The resulting marginal distributions highlight the differences between the environmental conditions in the five sea areas. Figure 4 shows also the uniform sampling of headings χ, highlighting the differences in the final uniform distributions provided by the 5 independent random generation processes used to generate the environmental conditions.

The resulting set of $\boldsymbol{e}^*$ inputs is then used to perform N_s DP analyses solving the nonlinear optimisation problem in Eq.(5). Figure 5 shows the results of the DP analyses, visualising the I_{DP} function for all the N_s calculation per each geographic sea area. The results are reported considering the pairwise comparison of V_w, H_s and T_p. According to Eq.(12), the function I_{DP} has only value 0 or 1 either the DP system holds or not the position. Therefore, in Figure 5 it is directly possible to identify the critical combination of parameters for the DP system in the five different areas. The representation of I_{DP} as a function of T_p and H_s gives the same insight of the scatter diagram approach but in this case, being the wind no more fixed for the H_s-T_p couples and being the results comprehensive of χ variations there is no clear separations between regions with $I_{DP} = 1$ and $I_{DP} = 0$.

The evaluation of OP_{DP} requires to check whether the MC integration process has reached a sufficient level of convergence. This can be performed monitoring the relative differences between OP_{DP} values at consecutive integration

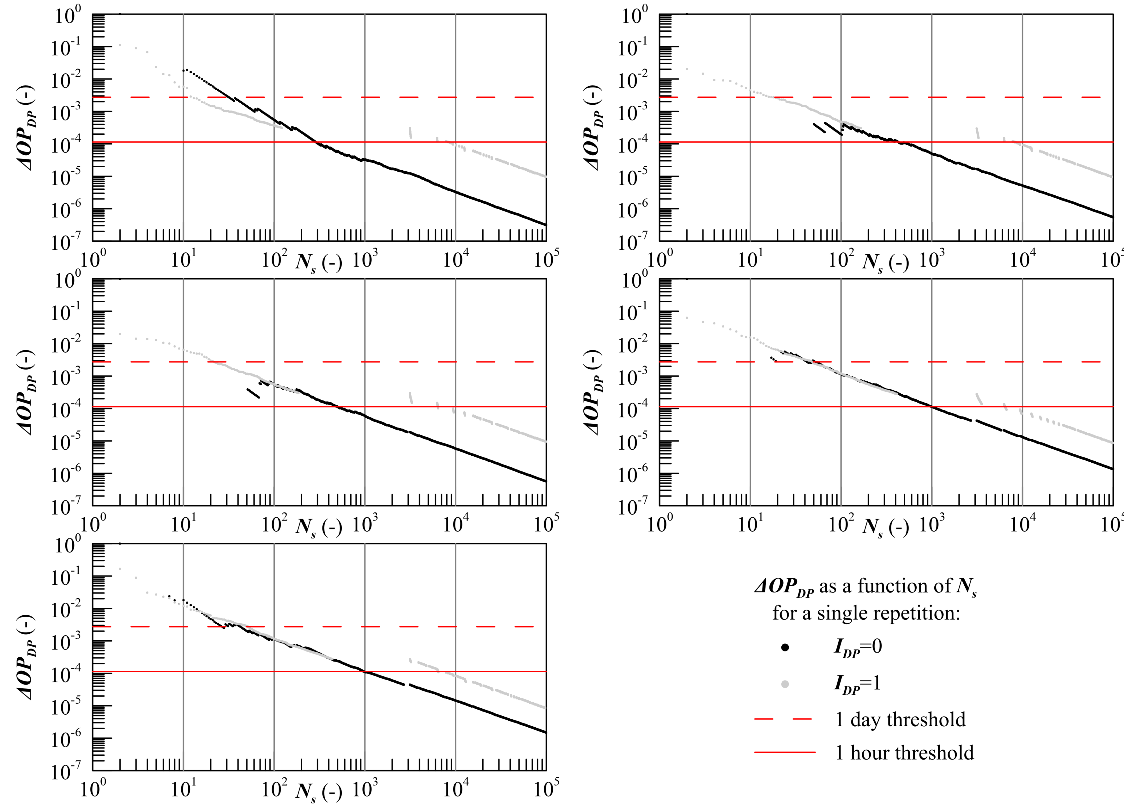

FIGURE 6. Convergence of MC process on a single OP_{DP} calculation for the five reference sea areas.

steps:

$$\Delta OP_{DP_i} = \left| \sum_{j=1}^{i} \frac{I_{DP_j}}{i} - \sum_{j=1}^{i-1} \frac{I_{DP_j}}{i-1} \right| \tag{23}$$

It is than necessary to compare the ΔOP_{DP} with a reference threshold value significant for the analysed problem convergence. Being the OP_{DP} a quantity defined between 0 and 1 that indicates the fraction of year a vessel could operate in a sea area at a given encounter angle, the convergence should be related to the time unit used to quantify the operability. In case it is quantified in days, considering 1 day as convergence threshold, the convergence can be reached when ΔOP_{DP} approaches $2.74{\cdot}10^{-3}$. Considering a threshold of 1 hour, then the ΔOP_{DP} of reference is $1.144{\cdot}10^{-4}$.

Figure 6 shows the OP_{DP} variations with N_s for the 5 reference geographic sea areas in logarithmic scale. It is possible to observe in all the subplots two distinct series of data, one corresponding to the results with $I_{DP} = 1$ and the other with $I_{DP} = 0$. As I_{DP}, the integrating function, has only two possible discrete values, the ΔOP_{DP} curve has two distinct trends and, consequently, the convergence should be checked on the higher sequence of points in the reference N_s range. Figure 6 shows also the two convergence thresholds corresponding to 1 day and 1 hour. It can be observed that for the 5 areas the 1 day threshold is reached with less than 100 samples, while satisfying the 1 hour threshold requires almost 10^4 samples for all the tested cases.

However, to consider the convergence of a single calculation may be misleading for the MC integration due to the fact that the MC process is subject to uncertainties. Therefore, for the estimation of the OP_{DP} it is advisable to perform multiple repetitions N_r to evaluate the DP operability within a confidence interval CI. Generally, when N_r is sufficiently high, a CI can be described by a normal distribution. Here, the OP_{DP} is analysed with $N_r = 10$, suggesting to employ the following formulation for CI:

$$CI\,(c) = \mu \pm t \frac{\sigma}{\sqrt{N_r}} \tag{24}$$

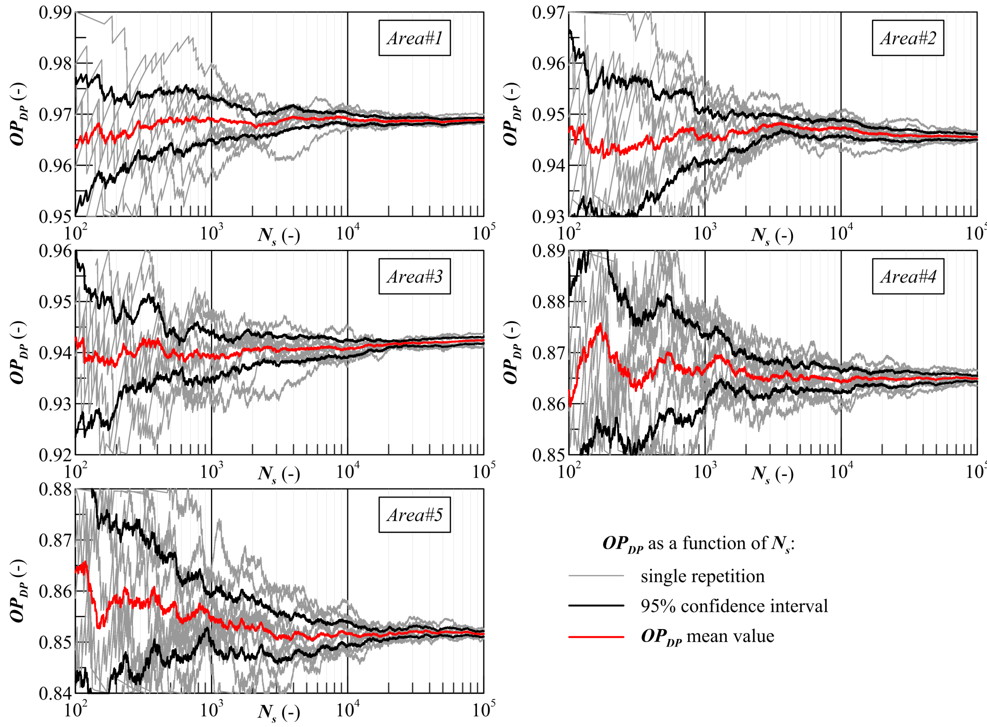

FIGURE 7. Solution history of OP_{DP} in the five selected areas with $N_r = 10$.

TABLE IV. OP_{DP} mean values μ and CI for the five reference sea area considering $N_r = 10$ and different N_s values.

N_s		*Area#1*	*Area#2*	*Area#3*	*Area#4*	*Area#5*
$1 \cdot 10^3$	μ	0.96910	0.94550	0.93930	0.86680	0.85470
	$CI(95\%)$	±3.76E-3	±4.75E-3	±4.32E-3	±6.40E-3	±4.45E-3
$5 \cdot 10^3$	μ	0.96906	0.94726	0.94086	0.86556	0.85094
	$CI(95\%)$	±1.55E-3	±1.66E-3	±2.14E-3	±2.33E-3	±3.19E-3
$1 \cdot 10^4$	μ	0.96909	0.94719	0.94075	0.86424	0.85161
	$CI(95\%)$	±1.11E-3	±1.53E-3	±1.58E-3	±1.94E-3	±2.24E-3
$5 \cdot 10^4$	μ	0.96844	0.94572	0.94198	0.86466	0.85197
	$CI(95\%)$	±5.07E-4	±6.62E-4	±8.36E-4	±9.96E-4	±6.94E-4
$1 \cdot 10^5$	μ	0.96844	0.94550	0.94244	0.86488	0.85162
	$CI(95\%)$	±3.92E-4	±4.99E-4	±5.83E-4	±5.14E-4	±5.28E-4

where μ is the mean value of OP_{DP} in the N_r repetition, σ is the repetitions variance and t is the inverse cumulative density function of of the Student t-distribution with confidence interval c and $N_r = 1$ degrees of freedom. Here, a 95% CI has been selected for the OP_{DP} estimation.

Figure 7 shows the OP_{DP} value as a function of N_s on the 5 reference geographic sea areas. The drawing reports the 10 repetitions together with the variation of the mean value μ, and the confidence interval CI. It can be observed that, as expected, the confidence interval CI reduces by increasing N_s for all the reference cases. However, comparing the CI values with the 1 day and the 1 hour thresholds, the convergence of the process is different than what observed for a single repetition. In fact, none of the selected cases reaches a CI beyond the 1 hour threshold, even considering all $N_s = 10^5$ samples. The 1 day threshold is reached for different N_s values depending on the sea area of reference, ranging from 1540 in *Area#1* to 6327 in *Area#5*. Table IV reports the mean value μ and the CI for the OP_{DP} evaluated in the 5 areas with different N_s. From the results it can be derived that the areas where the CI goes beyond the 1 day thresholds with less samples corresponds to the ones having higher OP_{DP}.

The OP_{DP} values obtained in the considered geographic sea areas are different between each other of more than 10%, highlighting the importance to perform DP predictions specific for the operational area of interest for the vessel.

This area-specific DP prediction increases the calculation time compared to a conventional capability analysis, as any single repetition for one sea area requires about 20 minutes of calculation time with $N_s = 10^5$. However, such a calculation effort is acceptable for DP analyses and ship design purposes. An improvement of the procedure can be obtained using different sample techniques for the joint distributions [18] that will speed up the convergence of the integral, thus decreasing the calculation time.

CONCLUSION

The present work implements a methodology based on MC integration to perform area specific DP predictions, starting from the modelling of environmental parameters with joint trivariate distributions. The adoption of such trivariate distributions does no more allow for the execution of a standard DP capability analysis, but requires the development of a specific process to determine the operability of the DP system in the geographic sea area. The application of the process on a reference OSV for five different sea areas highlight the importance of perform dedicated prediction for area-specific operations, as the operability value varies of more than 10% for the tested cases. The analyses performed on the convergence of the solution highlights that with the adopted number of samples and repetitions, operability can be determined within a confidence interval of 1 day in one year of operations. The area-specific DP prediction can be further improved by performing additional studies on the sampling process employed to determine the environmental random variables, aiming at a reduction of the results variance, thus of the calculation time. Finally, the newly proposed MC method increases the reliability of the environmental modelling for DP predictions, which is a significant improvement for practical engineering application of offshore industry.

REFERENCES

1. ABS, "Guide for dynamic positioning systems," Tech. Rep. (American Bureau of Shipping, 2014).
2. DNV, "Rules for classification of ships," Tech. Rep. (Det Norske Veritas, 2011).
3. DNV, "Dnv-st-0111 assessment of station keeping capability of dynamic positioning vessels," Tech. Rep. (Det Norske Veritas, 2021) edition December 2021.
4. IMCA, "Imca m 140 rev. i specification for dp capability plots," Tech. Rep. (The International Marine Contractors Association, 2000).
5. DNV, "Dnv rp c205 environmental conditions and environmental loads," Tech. Rep. (Det Norske Veritas, 2014).
6. F. Mauro and J. Prpić-Oršić, "Determination of a dp operability index for an offshore vessel in early design stage," Ocean Engineering **195**, 106764 (2020).
7. K. Johannessen, T. Meling, and S. Haver, "Joint distribution for wind and waves in the north sea," in *Proceedings of ISOPE 2001* (Stavanger, Norway, 2001).
8. F. Mauro and R. Nabergoj, "Advantages and disadvantages of thruster allocation procedures in preliminary dynamic positioning predictions," Ocean Engineering **123**, 96–102 (2016).
9. A. Aalberts, R. Kuipers, F. van Walree, and R. Jansen, "Developements in dynamic positioning systems for offshore stationkeeping and offloading," in *ISOPE Conference* (1995).
10. I. Wang, J. Yang, and S. Xu, "Dynamic positioning capability analysis for marine vessels based on dpcap polar program," China Ocean Engineering **32**, 90–98 (2018).
11. O. Smogeli, N. Trong, B. Borhaug, and L. Pivano, "The next level dp capability analysis," in *Dynamic Positioning Conference* (2013).
12. F. Mauro and F. Gaudiano, "Station-keeping calculations in early design stage: Two possible approaches," in *Proceedings of NAV 2018 Conference* (2018).
13. J. Balchen, N. Jenssen, and S. Saelid, "Dynamic positioning using kalman filtering and optimal control theory," in *IFAC/IFIP Symposium on the Automation in Offshore Oil Field Operation* (1976).
14. F. Mauro, A. Benci, V. Ferrari, and E. Della Valentina, "Dynamic positioning analysis and comfort assessment for the early design stage of large yachts," International Shipbuilding Progress **68**, 33–60 (2021).
15. F. Mauro and R. Nabergoj, "A global operability index for offshore vessel," in *Proceedings of the International Conference on Offshore Mechanics and Arctic Engineering - OMAE*, Vol. 1 (2020).
16. J. Hammersley and D. Handscomb, *Monte Carlo Methods* (Methuen & co. LTD, 1964).
17. L. Li, Z. Gao, and T. Moan, "Joint environmental data at five european offshore sites for design of combined wind and wave energy devices," in *Proceedings of the ASME 2013 32nd International Conference on Ocean, Offshore and Artic Engineering OMAE 2013* (Nantes, France, 2013).
18. F. Mauro and D. Vassalos, "The influence of damage breach sampling process on the direct assessment of ship survivability," Ocean Engineering **250**, 111008 (2022).